Pergamon

Int. J. Multiphase Flow Vol. 23, No. 6, pp. 1111–1129, 1997

Printed in Great Britain

PII: S0301-9322(97)00031-1

0301-9322/97 $17.00 + 0.00

THE EFFECTS OF INCLINATION ANGLE ON FLOODING IN A HELICALLY FLUTED TUBE WITH A TWISTED INSERT

Y. T. KANG[1]†, R. STOUT[2] and R. N. CHRISTENSEN[2]

[1]Department of Mechanical Systems Engineering, Tokyo University of Agriculture and Technology, 24-16, nakamachi, 2-Chome Koganei, Tokyo 184, Japan

[2]Department of Mechanical Engineering, The Ohio State University, 206 W. 18th Ave., Columbus, OH 43210, U.S.A.

(Received 5 April 1996; in revised form 15 April 1997)

Abstract—This paper develops an experimental flooding correlation as a function of the inclination angle for a fluted tube with a twisted insert for application to absorption heat pump systems. Fluted tubes have been used to enhance both heat and mass transfer during absorption and desorption processes. In the present tests, a plastic twisted tape was inserted to increase the absorption rate in counter current absorption. The effects of the twisted insert and the angle of inclination on flooding were examined. Water–ethyl alcohol solution flows downward in the fluted tube while air flows counter current in an upward direction. The flooding mechanism in a fluted tube with a twisted insert was analyzed by visual observation, and experimental correlations for flooding for both vertical and nearly horizontal tubes were developed. The experimental data from this paper were compared with those for smooth tubes from the literature. The results show that flooding was initiated from the top for inclination angles less than 60° while it started from the bottom of the tube for the angles larger than 60°. The fluctuation in pressure drop was very strong when flooding started from the bottom while it was not as strong when it started from the top. The effect of the position of the insert was not significant for the nearly horizontal tube while it had some effect for the vertical tube. For the fluted tube with an insert, the flooding vapor velocity was the highest for the inclination angle between 40° and 60° for superficial liquid velocities less than 1.178×10^{-2} m/s. When the superficial velocity of liquid flow is higher than 1.178×10^{-2} m/s, the superficial flooding vapor velocity increases with an increase of the inclination angle. © 1997 Elsevier Science Ltd.

Key Words: flooding vapor velocity, inclination angle, helically fluted tube, twisted insert, air–water and ethyl alcohol

1. INTRODUCTION

Flooding occurs in many different applications such as falling film evaporators, packed columns, nuclear reactors, and vertical tube condensers. In counter-current flows, as the vapor velocity gradually increases for a given tube geometry and liquid–gas pair, a point is reached where large waves and disturbances occur at the interface, resulting in a chaotic flow pattern near the bottom of the tube with the liquid film being held up or entrained by the upward gas flow. This point is known as the onset of flooding. The minimum vapor velocity at which flooding occurs is known as the flooding vapor velocity.

To describe the onset of flooding in vertical counter-current flow, many empirical correlations have been suggested: Wallis (1961), Clift *et al.* (1966), Cetinbudaklar and Jameson (1969), Maron and Dukler (1984), etc. Imura *et al.* (1977) reviewed seven experimental correlations for the flooding velocity and provided a theoretical correlation based on instability and the experimental data. Dukler and Smith (1979) proposed five flow regimes in transition to flooding from stable counter-current flow. The following flow regimes depend on the flow rate of liquid and gas, geometry of the tube and the orientation of the tube as shown in figure 1: slugging, bridging, liquid entry, standing-wave and hanging film regions. Since the interfacial wave of a very thin liquid film is not big enough to cause slugging or bridging inside the tube, flooding at low liquid flow rates

†To whom correspondence should be addressed.

is characterized by either hanging film or standing-wave. A hanging film is caused by the pressure of the upward gas flow while standing-wave is caused by an agitated interface. At moderate liquid flow rates, the flooding point moves from the liquid exit (bottom) to the liquid entrance (top). In standing-wave regime, the flooding phenomenon is initiated suddenly with the liquid churning below the liquid entrance. When the liquid flow becomes large enough to allow a large wave at the interface, flooding is characterized by either slugging or bridging of the liquid film. Taitel and Barnea (1982) presented a film model to predict flooding and flow reversal process for gas–liquid flow in vertical tubes. The theory requires an expression for the interfacial shear as an input.

McQuillan and Whalley (1985) described the compilation of a data bank containing 2762 experimental flooding data points, and compared 22 empirical flooding correlations using dimensionless superficial velocities. They recommended the correlation presented by Alekseev *et al.* (1972) as the most accurate correlation. Bankoff and Lee (1986) reviewed the flooding literature, and summarized the characteristics of the flooding phenomenon as a sudden increase in pressure drop, appearance of large disturbance waves at the gas-liquid interface and entrainment of liquid droplets. They summarized the eight analytical models and 14 empirical correlations of flooding for vertical counter-current flows. These models and the empirical correlations are based on the smooth tube with air and various liquids, mostly water. Recently, Lacy and Dukler (1994a, 1994b) performed experimental and numerical studies of flooding in the liquid entry region using a porous plastic tube, and suggested that flooding occurs when the interfacial shear is sufficiently high to cause a reversal in the direction of the velocity at the surface of the film.

Some literature on flooding in horizontal or inclined tubes has also been found. Lee and Bankoff (1983) developed a theory for the onset of flooding in inclined stratified flow based on the hydrodynamic and energy equations for condensing flow. They proposed that condensation has little effect on the onset of flooding if flooding is initiated at the bottom of the tube. Barnea *et al* (1986) investigated the effect of the liquid injection mode on flooding in nearly horizontal tubes, and observed that the porous injection system causes a local disturbance and enhances flooding at relatively shallow inclinations and high liquid flow rates. In the case of stratified flow, Taitel and Dukler (1976) presented a criterion for an unstable interface at which the wave will grow and the liquid will be swept into the gas flow in the form of a slug or waves. Recently, Choi and No (1995) examined the effects of the pipe diameter, end geometry, and inclination angle on flooding. They categorized the mechanisms of the onset of flooding into two groups: 'inner flooding' and 'entrance flooding'. In the case of inner flooding, flooding is initiated by sudden wave growth and characterized by slug formation. The inclination angle is one of the important parameters

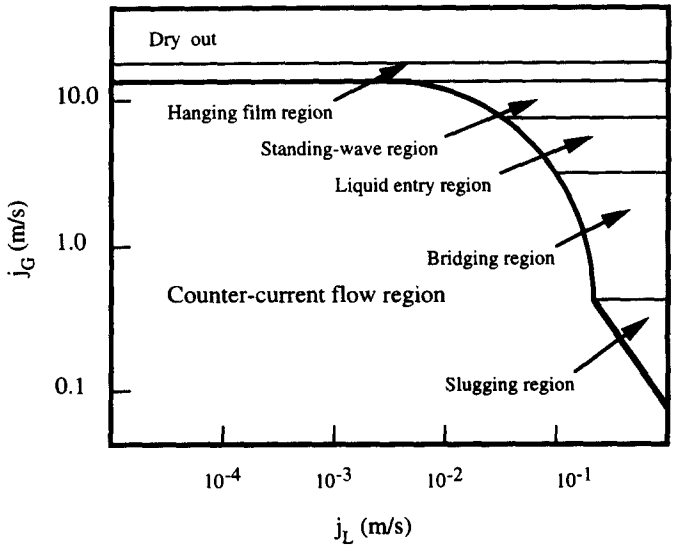

Figure 1. Flooding regimes for vertical counter-current flows (Dukler and Smith 1979).

governing flooding in nearly horizontal tubes. In the case of entrance flooding, no slug formation occurs.

Most flooding data were obtained for flat plates or smooth tubes. In many thermal applications such as absorption heat pump systems, fluted tubes have been recommended to increase heat and mass transfer rates and heat transfer area per unit volume (Srinivasan and Christensen 1992; Garimella and Christensen 1995; Kang *et al.* 1996). Flutes in the fluted tube break the boundary layer at every pitch so that heat transfer coefficient is very high in the fluted tube. It was also found that the vapor velocity should be maximized to have a high absorption rate for counter current absorber (Kang and Christensen 1994; Herbine and Perez-Blanco 1995). Therefore, it is required to use the fluted tube and the insert to increase heat and mass transfer coefficients and the contact time between the liquid and vapor in the fluted tube during the counter current absorption/desorption process. As the vapor velocity increases, flooding or liquid back flow can occur in counter-current flow. The liquid back flow significantly degrades heat and mass transfer performance in these absorption systems. However, no flooding data and/or correlations for the fluted tube have been found in the literature. Therefore, it is required to study the flooding process and develop a correlation for flooding in counter current flow systems with fluted tubes.

In this paper, the flooding mechanism in a fluted tube with a twisted insert was investigated and the effects of the insert, tube geometry and the inclination angle on the flooding vapor velocity were considered. Experimental data for fluted tubes were analyzed and compared with existing literature for smooth tubes. The experimental correlations for the flooding vapor velocity were developed as a function of the angle of inclination.

2. EXPERIMENTAL APPARATUS AND PROCEDURE

Figure 2 shows a schematic diagram of the experimental apparatus. A water and ethyl alcohol solution (30% ethyl alcohol by weight) flows downward in a fluted tube while air at atmospheric pressure flows counter current to the liquid in an upward direction. Viscosity and surface tension of the ethyl alcohol solution are 2.662×10^{-3} N-s/m^2 and 33.0 dyne/cm, respectively. The design of the upper plenum was such that the liquid was introduced into the annular area between the plenum shell and the center tube. The liquid then flows up within the annulus before going over the edge of the center tube and down into the fluted tube. Vee notches were cut into the top of the center tube above each start of the fluted tube to distribute the liquid. The notches worked well for the vertical case but became less effective for off vertical cases. Air was removed from near the top of the plenum and sent to the surge tank. This allowed for the recovery of any liquid carryover. The lower plenum can be thought of as an upside down version of the upper plenum. Liquid draining out of the test section pools in the bottom of the plenum and then flows back to the liquid surge tank. Sufficient liquid was maintained, as viewed in the sight glass, in the plenum to prevent air from leaving with the liquid. The air was introduced into the upper section of the lower plenum in the annulus between the plenum shell and the center tube. It then flowed down through the annulus until it reached the bottom of the center tube. At this point, it entered the center tube and flowed up through the test section. The transparent fluted tubes were made by using a chemical etching process.

The pressure drop was measured using a water U-tube manometer. The pressure taps were located within the air space of the top and bottom plenums. Liquid and air flowmeters were used to measure both liquid and air flow rates. The liquid meter was calibrated for water and ethyl alcohol and care was taken to minimize the back pressure on the air flow meter. The inclination angle from the horizontal axis was measured using a machinists protractor. The uncertainty for the experiments arose from data reading (reading error) and calibration of flow meters (calibration error). The reading errors from the liquid flow meter, air flow meter, the tube diameter and the inclination angle were 2.89, 0.59, 0.1, and 1.87%, respectively. The calibration error for liquid flow meter was 4.0% in conversion from water to water–ethyl alcohol solution. Therefore, the uncertainty of the flooding correlation provided by the present paper is 5.31%, which was obtained by using Moffat's method (Moffat 1988).

For a given configuration, the desired liquid flow rate was established first while maintaining

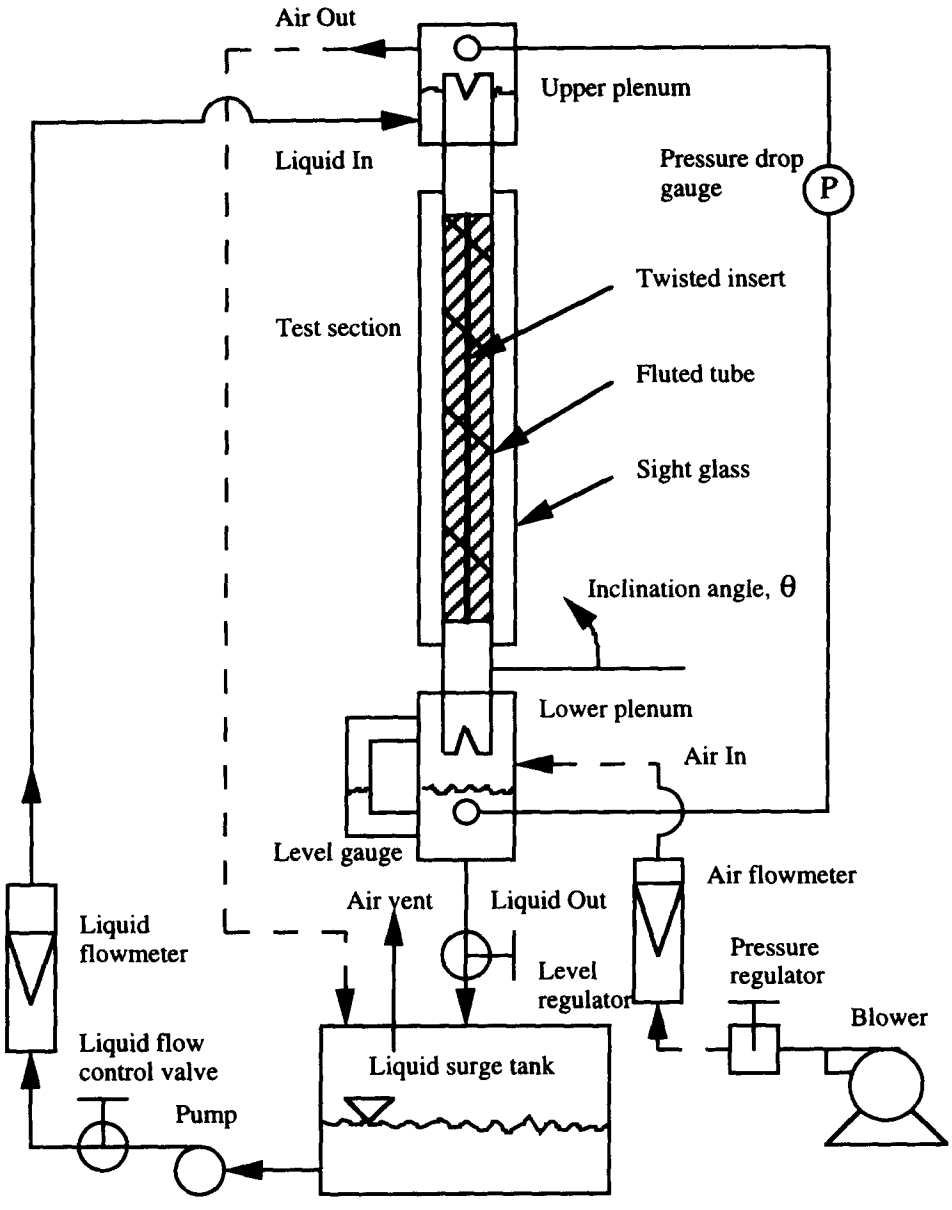

Figure 2. Schematic diagram of the experimental apparatus.

some low air flow rate. Subsequently, the air flow rate was slowly increased until flooding occurred. The pressure drop across the test section was used to define the onset of the flooding. As the air flow rate increased, the pressure drop increased. The pressure drop was very steady at any given air flow rate below the flooding point. Once flooding started, the pressure drop became very erratic. The onset of fluctuation in the pressure drop was used as the indicator of flooding. Data were taken for angles of inclination of 1,.5, 10, 30, 45, 60, 75, 85 and 90° from the horizontal axis. For each inclination angle, data were taken for several liquid flow rates in order to define a flooding curve for that angle. To simplify correlating the flooding vapor velocity and the inclination angle, data were taken for a predetermined set of liquid flow rates.

Figures 3 and 4 represent the schematic diagrams of the fluted tube and the twisted insert used in this paper. In the present experiments, the geometric conditions of the fluted tube and the twisted insert were kept constant. The fluted tube has geometric dimensions of $D_{ei} = 1.44D_{bi}$, $N_S = 5$, pitch $= 0.47D_{bi}$, where D_{bi}, D_{ei}, N_S are the inner bore diameter, the inner envelope diameter, and the number of starts of the fluted tube, respectively. The twisted insert has the geometric dimensions

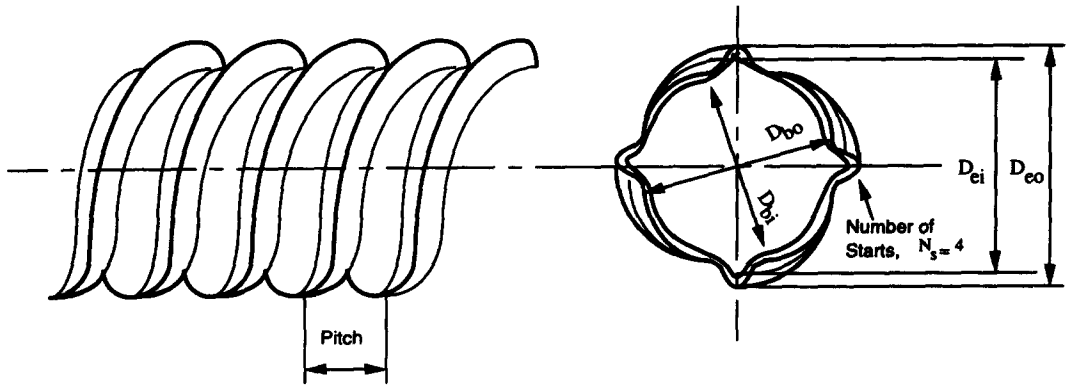

Figure 3. Definition of geometric parameters of a fluted tube.

of $A = D_{bi}$, $B = 1.536D_{bi}$, $C = 0.266D_{bi}$ and $D = 0.0923D_{bi}$, where A, B, C and D are defined in figure 4. D_{bi} is order of 25 mm and the length of the tube is 606.7 mm. The length of the insert is equal to the tube length. The hydraulic diameter of the test section, D_h, was calculated based on the definition for the noncircular tube ($4A_c$/perimeter) by considering the air passage in helical direction. Figure 5 shows the fluted tube with a twisted insert when air is not introduced from the bottom of the test section. As can be seen in figure 5, the insert was twisted in opposite direction to the helix angle of the fluted tube so that the vapor flow helped wet the surface.

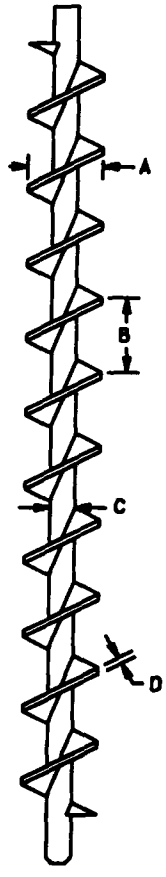

Figure 4. Schematic diagram of the twisted insert.

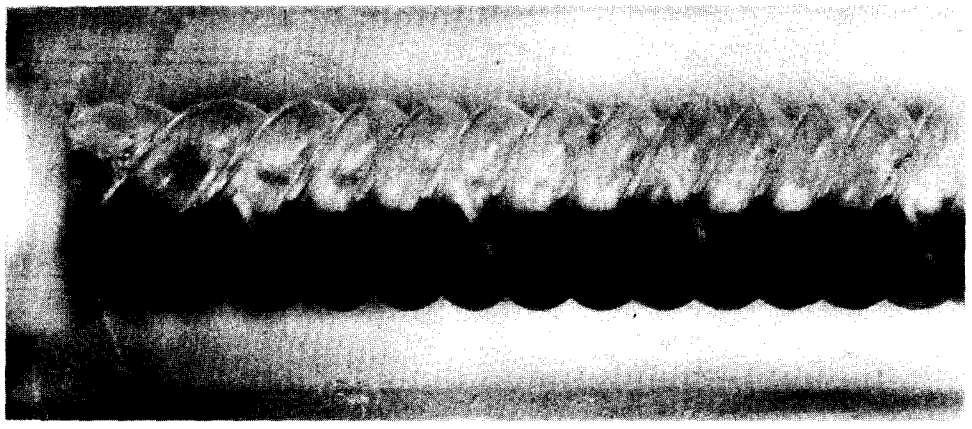

Figure 5. The fluted tube and the twisted insert without air flow.

3. RESULTS AND DISCUSSIONS

3.1. *Visual observations*

Generally, the flooding condition is reached either by gradually increasing the vapor flow rate for a given liquid flow rate or vice versa. In this paper, the flooding conditions were obtained by increasing the vapor flow rate for a fixed liquid mass flow rate. The onset of flooding has been defined differently by many authors. Wallis (1961) defined the onset of flooding as the point where the liquid flow became chaotic with large amplitude waves near the interface. Hewitt and Wallis (1963) defined it as the point where the liquid was expelled to the top of the tube. In components of absorption heat pump systems, chaotic flow is required to have more mixing without any liquid carryover to the top of the tube (inlet of the liquid flow). Therefore, in the present paper, the flooding point defined by Hewitt and Wallis (1963) was followed.

The onset of flooding was detected by both visual observation and monitoring the pressure drop. When the air flow rate was increased, the pressure drop also increased very slowly. As the air flow rate neared the flooding condition, the pressure drop increased somewhat faster than the unflooded condition, and finally started to fluctuate at the flooding point. Figure 6(a) represents the flow patterns for the vertical fluted tube with a twisted insert (90° condition). Very stable annular flow was reached at the unflooded stage as shown in (a) of figure 6(a). Just before the flooding point, the pressure drop remained constant for a while without any fluctuation. Numerous bubbles were activated at the bottom as shown in (b) of figure 6(a). Just after the flooding point, the pressure drop started to fluctuate due to the flow fluctuation from the bottom of the tube and the liquid carryover to the top of the tube. Some liquid was held up at the location of the flooding point, and the liquid flow rate at the outlet of the tube decreased suddenly at this stage. Vapor slugs were formed in the core region, the interface wave fluctuated significantly and the flow became chaotic as shown in (c) of figure 6(a). Figure 6(b) represents the flow patterns for the nearly horizontal fluted tube with a twisted insert (1° condition). Initially, stable stratified flow developed. The gas/liquid interface started to incline due to the air flow from the bottom as shown in (a) of figure 6(b). Just before flooding, a hydraulic jump was formed gradually at the top of the tube (liquid inlet) as shown in (b) of figure 6(b). At the flooding point, a very sharp hydraulic jump was generated near the liquid inlet end of the tube. This jump quickly moved upstream toward the liquid inlet and disappeared. This cycle was repeated continuously with liquid carryover. The flow pattern downstream of the flooding point was relatively stable as shown in (c) of figure 6(b).

Figure 7 represents the onset of flooding in a fluted tube with an insert for each inclination angle. The onset of flooding changed from the top to the bottom of the tube at a transition condition (an inclination angle of 60° and a superficial velocity of liquid flow, j_L of 5.50×10^{-3} m/s). When flooding starts from the top, the flooding region propagates slowly to the bottom. Especially, for a nearly horizontal tube, the flooding region covered less than one fourth of the tube length from the top. The flooded region increased as the inclination angle increased until 30°, at which the entire tube was flooded. When flooding starts from the bottom, the flooding point propagates very rapidly

to the top, and the entire tube is flooded almost at the same time. The fluctuation in the pressure drop was very strong when flooding started from the bottom because the flooding point moved up to the top very rapidly, and fluctuated up and down through the test section. However, the pressure drop fluctuation for the nearly horizontal tubes was not as strong as those for the inclination angles larger than 60°. This weak fluctuation for the nearly horizontal tube was caused by only the liquid carryover to the top and flooding did not propagate to the bottom but remained near the top of the tube. However, the strong fluctuation was caused by both the liquid carryover and the flow fluctuation itself when the flooding started from the bottom.

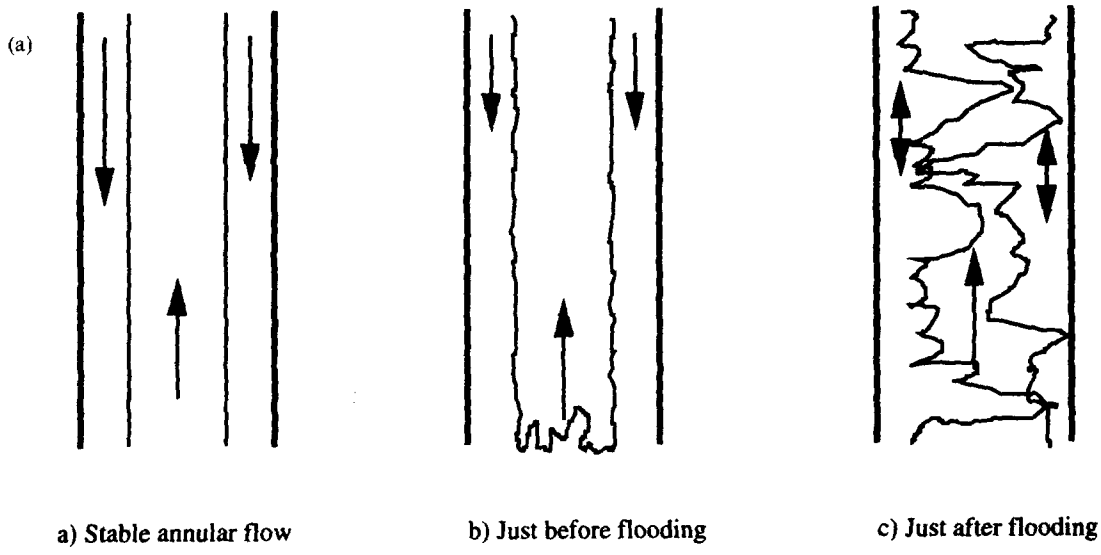

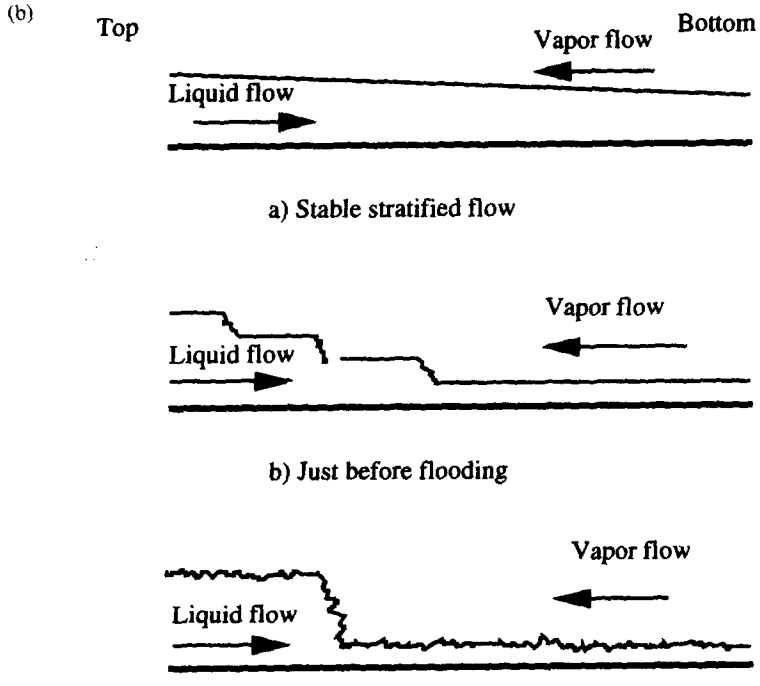

Figure 6. (a) Flow patterns for the vertical fluted tube with an insert. (b) Flow patterns for the nearly horizontal fluted tube with an insert.

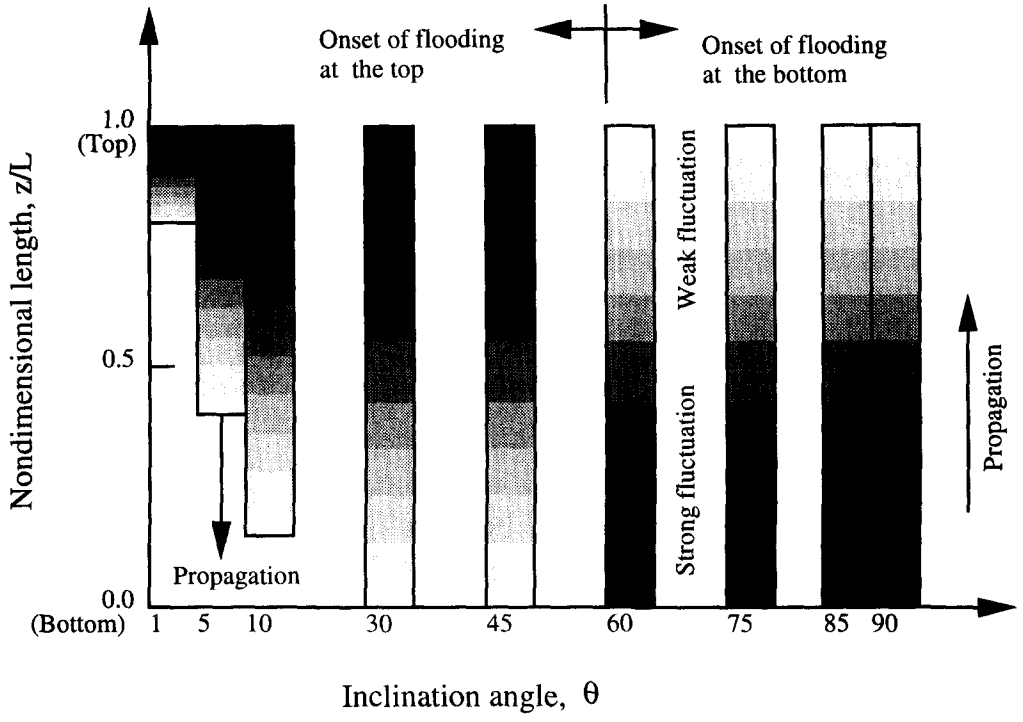

Figure 7. Onset of flooding for the fluted tube with an insert.

3.2. *Flooding curve for each inclination angle*

Figure 8 shows the flooding curves in the fluted tube with a twisted insert for each inclination angle. The slope of the flooding curve becomes flatter as the inclination angle increases. This implies that the flooding vapor velocity is more sensitive to the liquid flow rate for the horizontal position than for the vertical position.

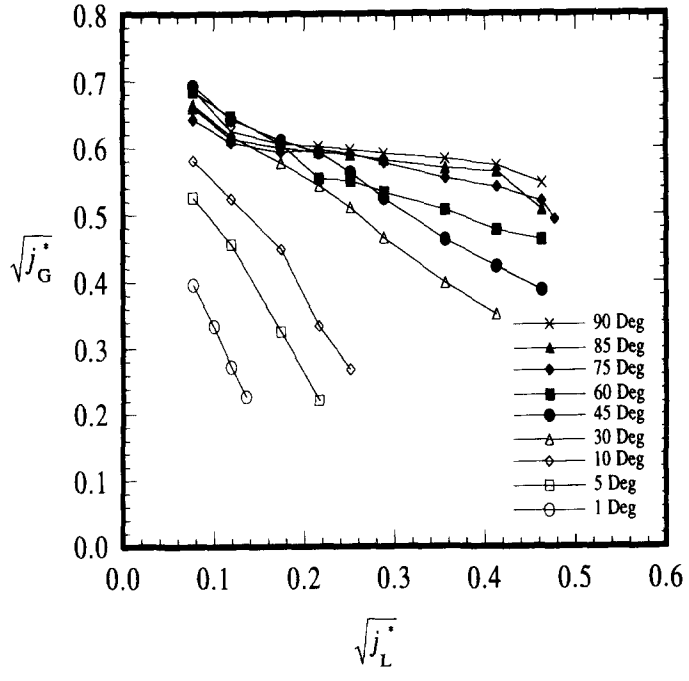

Figure 8. Flooding curves for the fluted tube with a twisted insert.

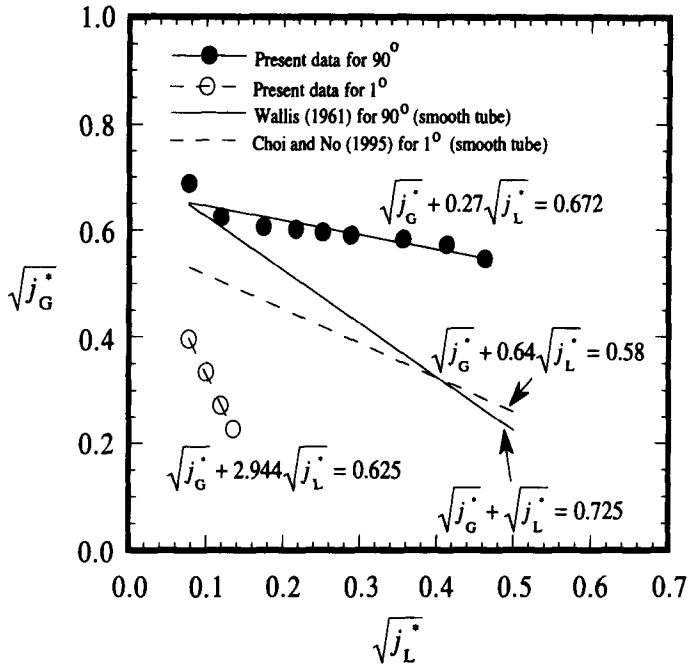

Figure 9. (a) Flooding curve for the vertical fluted tube with an insert. (b) Flooding curve for the nearly horizontal fluted tube with an insert.

Figure 9 shows a comparison of the flooding curves for the fluted tube with a twisted insert with those for the smooth tube in both vertical and nearly horizontal positions. The flooding correlation by Wallis (1961) for vertical smooth tubes was compared with the present data for the vertical fluted with a twisted insert. Wallis (1961) correlated the flooding data with dimensionless parameters as follows

$$\sqrt{j_G^*} + \sqrt{j_L^*} = 0.725, \qquad [1]$$

where

$$j_G^* = \frac{j_G \rho_G^{1/2}}{\sqrt{gD_h(\rho_L - \rho_G)}} \quad \text{and} \quad j_L^* = \frac{j_L \rho_L^{1/2}}{\sqrt{gD_h(\rho_L - \rho_G)}} \qquad [2]$$

In [2], j is superficial velocity, ρ density, g acceleration due to gravity, D_h hydraulic diameter, subscripts L and G are liquid and vapor (gas), respectively. The Wallis correlation (1961) was obtained for tube aspect ratios (L/D) of 96.1, 64.2, 48.0 and 23.9 for an air–water mixture. The present data were obtained for a tube aspect ratio of 24.5 for an air–water/ethyl alcohol mixture. The present data were correlated by the following equation as shown in figure 9

$$\sqrt{j_G^*} + 0.27\sqrt{j_L^*} = 0.672. \qquad [3]$$

The slope of the present correlation is less than that of the Wallis correlation. Figure 9 shows that the superficial flooding vapor velocity for a fluted tube with a twisted insert is higher than that for the smooth tube from Wallis (1961) for a given mass flow rate of liquid. O'Brien *et al.* (1986) also obtained experimental flooding data for smooth tubes with a very similar trend to the current flooding data for the fluted tube. The flooding velocities for the fluted tube are somewhat higher than those for the smooth tubes (O'Brien *et al.* 1986) for the same ranges of j_L^*. Moreover, the flooding data started to flatten from $j_L^{*1/2}$ of 0.5 in O'Brien *et al.* (1986) while it started from $j_L^{*1/2}$ of 0.15 in the present data. This is mainly because the vapor flows directly upward for the smooth tube while in the fluted tube it flows upward with flow restriction due to the twisted insert. The other reason is that much of the liquid flows in the flutes where it is not affected by the air flow.

Choi and No (1995) developed the following correlation for nearly horizontal smooth tubes (0.23–0.92°) with tube aspect ratios of 22.5, 33.6, 45.0 and 90.4 for an air–water mixture

$$\sqrt{j_G^*} + 0.64\sqrt{j_L^*} = 0.58. \quad [4]$$

The present data for the nearly horizontal tube (1°) were correlated by the following equation

$$j_G^* + 2.944\sqrt{j_L^*} = 0.625. \quad [5]$$

As shown in figure 9, the slope from the present data for a fluted tube with an insert is larger than that from Choi and No (1995) for the smooth tube. The flooding vapor velocity from the present experiments is lower than that from Choi and No (1995) because flooding initiates at the inlet of the liquid flow and the insert restricts the liquid flow at the top. The liquid flowed down as a stratified flow with a flow restriction by the twisted insert at every pitch. The air flowed upward with a flow restriction by the flutes of the fluted tube and the twisted insert. The air flow was blocked by the liquid flow at every pitch of the insert near the top of the tube.

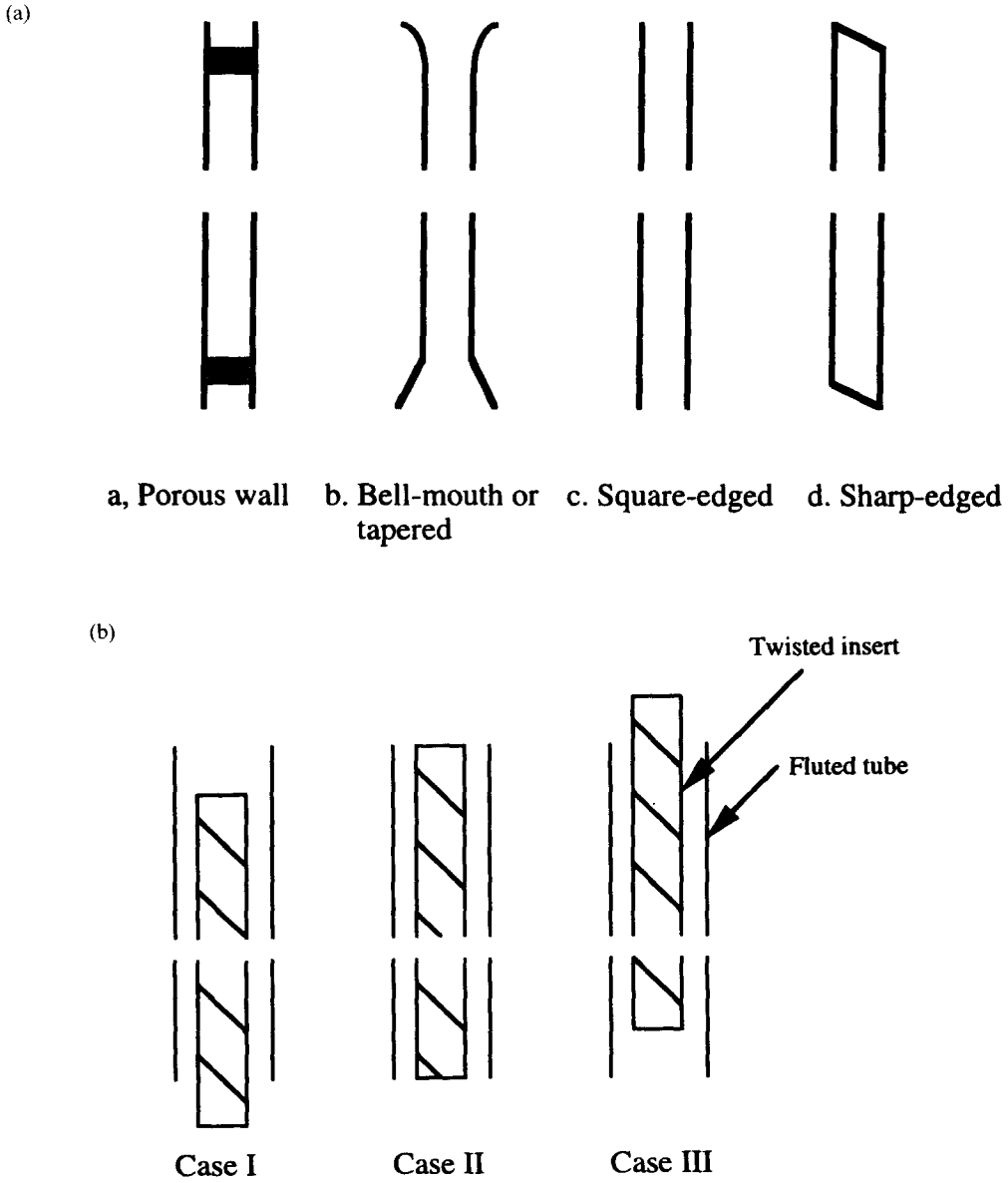

Figure 10. (a) Representative geometric configurations of the tube-ends. (b) Geometric configurations of tube-ends in the fluted tube with an insert.

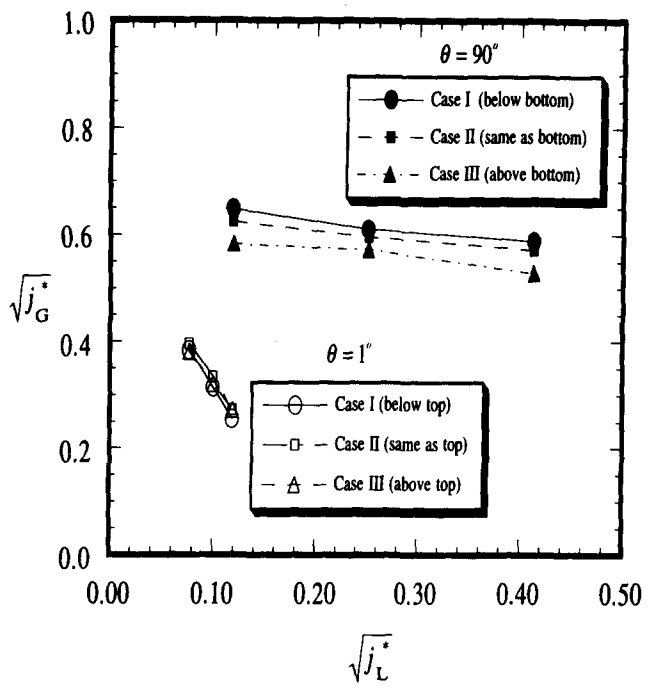

Figure 11. The effects of the position of the insert on the flooding.

3.3. The effects of the position of the insert

The onset of flooding is very sensitive to the geometry of the test section, and is especially sensitive to the configuration of the inlet and outlet (Bankoff and Lee 1986). The pitch of the twisted insert has relatively small effect on the onset of flooding compared with the tube end-conditions. Therefore, this paper investigates only the effect of the tube end-conditions on the onset of flooding. Imura *et al.* (1977) surveyed 10 different geometries of tube ends. Bankoff and Lee (1986) summarized 12 tube end-conditions adopted by various investigators. All the tube end-conditions used in the literature can be categorized into a combination of four representative shapes: (a) porous wall; (b) tapered or bell-mouth; (c) square-edged; and (d) sharp-edged conditions. For instance, Wallis (1961) used the square-edged inlet and outlet conditions while Pushkina and Sorokin (1969) used the bell-mouth inlet and square-edged outlet. Figure 10(a) shows the four representative configurations of the tube ends from the literature. Bankoff and Lee (1986) reported that the flooding vapor velocity for the porous wall condition is higher than that for the square-edged condition. Govan *et al.* (1991) also reported the flooding flow rate for the sharp-edged liquid outlet/vapor inlet conditions is much lower than that for the square-edged liquid outlet/vapor inlet conditions. The tapered conditions lie between the sharp-edged and the square-edged conditions. The geometry used in the present experiments may be added as the fifth category for the representative shapes, which is named 'enhanced surface tube with an insert'. Figure 10(b) shows the geometries of the tube end-conditions in the present experiments. The twisted insert ends below the top and bottom of the fluted tube in case I, ends at the same position as the fluted tube in case II, and ends above the top and bottom of the fluted tube in case III.

Figure 11 shows the effects of the tube end-conditions (the different position of the insert inside the fluted tube) on the flooding condition for vertical and nearly horizontal tubes. All the experimental data in the present paper were obtained from case II except figure 11. The effect of the position of the insert was not significant for the nearly horizontal tube while it was somewhat more significant for the vertical tube. However, the inlet conditions do not account for the difference shown in figure 9. As shown in figure 11 for the vertical position, the superficial flooding vapor velocity for case III (the position of the insert at above the top) is lower than that for case II, and case II has a lower superficial flooding vapor velocity than case I for a given mass flow rate of liquid flow. This was because the flooding initiated at the bottom for the vertical position.

Case III has an irregular end condition at the bottom due to the insert position above the liquid outlet. For the nearly horizontal position, the flow fluctuation was not strong because the flooding initiated at the top of the tube. Figure 11 shows that the superficial flooding vapor velocity for the nearly horizontal position is much lower than that for the vertical position for a given mass flow rate of the liquid flow.

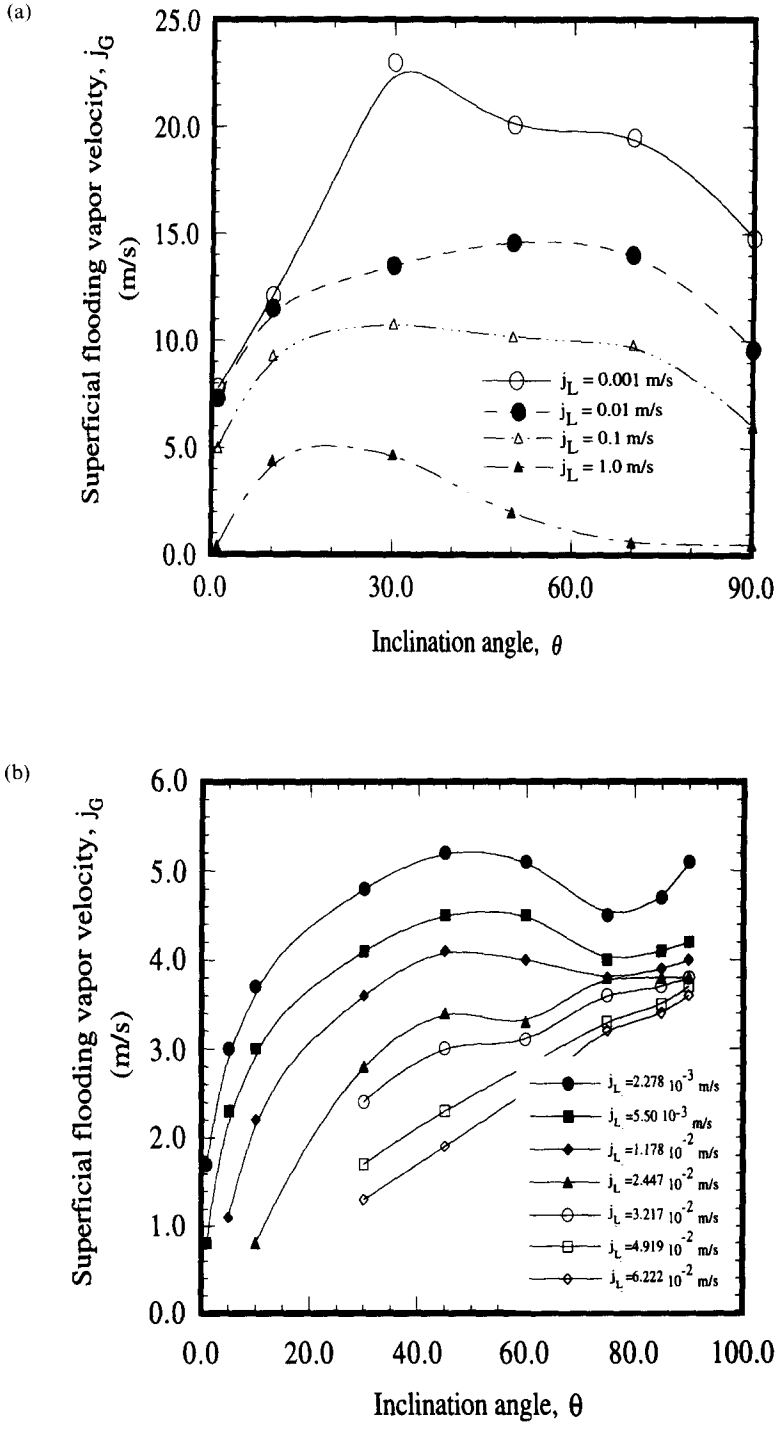

Figure 12. (a) Flooding vapor velocity vs inclination angle for each liquid velocity in a smooth tube (Barnea *et al.* 1986). (b) Flooding vapor velocity vs inclination angle for each liquid velocity in the fluted tube.

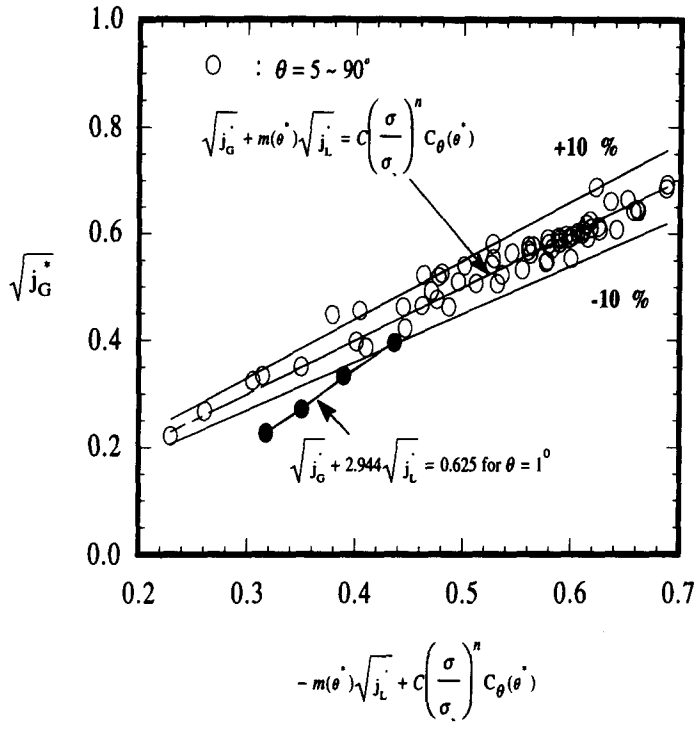

Figure 13. Flooding correlation including inclination angle.

3.4. *Effects of inclination angle*

Figure 12(a) and (b) show the effects on inclination angle on the flooding vapor velocity for the smooth tube and the fluted tube with an insert, respectively. Figure 11(a) was plotted by reading the data from figure 10 in Barnea *et al.* (1986), in which experimental data were obtained for a smooth tube, diameter of 51.0 mm with air and water. As can be seen in figure 12(a), the flooding vapor velocity is the highest between the inclination angles of 20° and 40°. The flooding vapor velocity is more sensitive to the inclination angle near horizontal position than near vertical position. Kawaji *et al.* (1991) also reported that the highest flooding vapor velocity might lie between 22.5° and 45° for the smooth tube. For the fluted tube with an insert as shown in figure 12(b), the flooding vapor velocity is the highest between the inclination angle of 40° and 60° for the superficial liquid velocities of 1.178×10^{-2} m/s and lower. When the superficial velocity of liquid flow is higher than 1.178×10^{-2} m/s, the superficial flooding vapor velocity increases with an increase of the inclination angle, and it increases linearly at superficial liquid velocities higher than 4.919×10^{-2} m/s.

3.5. *Experimental correlation*

Figure 13 represents the experimental correlation for a helically fluted tube with a twisted insert. Since figure 8 confirmed that the slopes of the flooding curves are strong functions of the inclination angle, the following functional form was used to develop the experimental correlation

$$\sqrt{j_G^*} + m(\theta^*)\sqrt{j_L^*} = C\left(\frac{\sigma}{\sigma_w}\right)^n C_0(\theta^*), \qquad [6]$$

where C is a constant to correlate the experimental data, and σ is surface tension of the liquid used and σ_w is that of water at room temperature (0.072 N/m). The constant, n, varies from 0.1 to 0.5 depending on the literature. In the present work, n was selected as 0.2 because the curves given by Boucher and Alves (1973) are consistent with an average of around 0.2 for n. All the experimental data between 5° and 90° were correlated by the following equations for m and C_0

with an error band of $\pm 10\%$

$$m(\theta^*) = 2.123 - 6.288\theta^* + 9.643\theta^{*2} - 5.358\theta^{*3}, \quad [7]$$

$$C_0(\theta^*) = 0.2262 + 0.2214\theta^* - 0.2048\theta^{*2}, \quad [8]$$

$$C = 2.226 \quad [9]$$

and

$$\theta^* = \frac{\theta}{90}, \quad [10]$$

where θ is the inclination angle from the horizontal axis. For the nearly horizontal position, the experimental data were not correlated by the above correlation but by [5]. Experimental ranges for the above correlation are $0.05 < j_G^* < 0.5$ and $0.006 < j_L^* < 0.23$.

3.6. Comparisons

Two different types of flooding correlation were compared with the present experimental data: one using a nondimensional parameter introduced by Wallis (1961) and the other using Kutateladze number. General expression of Wallis (1961) equation is given by

$$\sqrt{j_G^*} + m\sqrt{j_L^*} = C. \quad [11]$$

Originally, the form of this equation was obtained from experimental data. However, Wallis correlation can also be derived from the consideration of shear stress, momentum flux, and hydrostatic forces for each component of the fluid (Wallis 1969). It has been found by Butterworth (1992) that it is necessary to correct the Wallis equation for tube-ends effects and liquid surface tension. Butterworth (1992) proposed the following corrected equation for the effect of the surface tension

$$C = \sqrt{0.53F_1F_2}, \quad [12]$$

where

$$F_1 = \left(\frac{\sigma}{\sigma_w}\right)^n \quad [13]$$

and the correction factor F_2 is unity for a square-ended tube cut but can be greater for sharp-ended tubes. Some data for the correction factor F_2 are available in Butterworth (1992) for angled tube ends with different tube diameters.

Tien *et al.* (1980) correlated flooding data using Kutateladze number as follows

$$\sqrt{K_G} + m\sqrt{K_L} = C, \quad [14]$$

where

$$K_G = \frac{j_G\rho_G^{1/2}}{[g\sigma(\rho_L - \rho_G)]^{1/4}} \quad \text{and} \quad K_L = \frac{j_L\rho_L^{1/2}}{[g\sigma(\rho_L - \rho_G)]^{1/4}}. \quad [15]$$

This correlation is valid only for an extreme case, namely zero liquid penetration. Chung *et al.* (1980) obtained by experiments that $m = 0.65$–0.80 and C is a function of the nondimensional diameter, D^*, as follows

$$C = C_1 \tanh(C_2 D^{*1/4}) \quad [16]$$

and

$$D^* = \frac{D_h}{\sqrt{\dfrac{\sigma}{g(\rho_L - \rho_G)}}}, \quad [17]$$

where $C_1 = 1.79$–2.1 and $C_2 = 0.8$–0.9.

In actual components of the absorption heat pump systems such as absorbers, desorbers and rectifiers, which have counter-current flows between the liquid and the vapor, it is required to determine if the flooding phenomenon occurs or not for given thermal and geometric conditions of the component. Generally, the geometric conditions should be selected to avoid the flooding condition for a given ratio of the mass flow rate between the liquid and the vapor. Therefore, it is instructive to plot the superficial vapor velocity as a function of the ratio of the flow rates so that one can judge if flooding occurs or not for a given condition.

Wallis and Kutateladze-Tien correlations are rearranged as follows based on the above consideration

$$j_G = \frac{C^2\left[gD_h\frac{\rho_L-\rho_G}{\rho_G}\right]^{1/2}}{\left[1+m^{1/2}\left(\frac{\dot{m}_L}{\dot{m}_G}\right)^{1/2}\left(\frac{\rho_G}{\rho_L}\right)^{1/4}\right]^2} \quad \text{from Wallis correlation} \qquad [18]$$

and

$$j_G = \frac{C\left[g\sigma\frac{\rho_L-\rho_G}{\rho_G^2}\right]^{1/4}}{1+m\left(\frac{\dot{m}_L}{\dot{m}_G}\right)\left(\frac{\rho_G}{\rho_L}\right)^{1/2}} \quad \text{from Kutateladze–Tien correlation.} \qquad [19]$$

Figure 14 shows the superficial flooding vapor velocity as a function of the ratio of the liquid mass flow to the vapor mass flow for each inclination angle in the fluted tube with an insert. The flooding vapor velocity decreases as the ratio of mass flow rates increases. The effect of the ratio of mass flow rates on the flooding vapor velocity becomes more significant as the inclination angle decreases. Figure 14 also shows that the flooding vapor velocity becomes more sensitive to the ratio of mass flow rates as the ratio decreases.

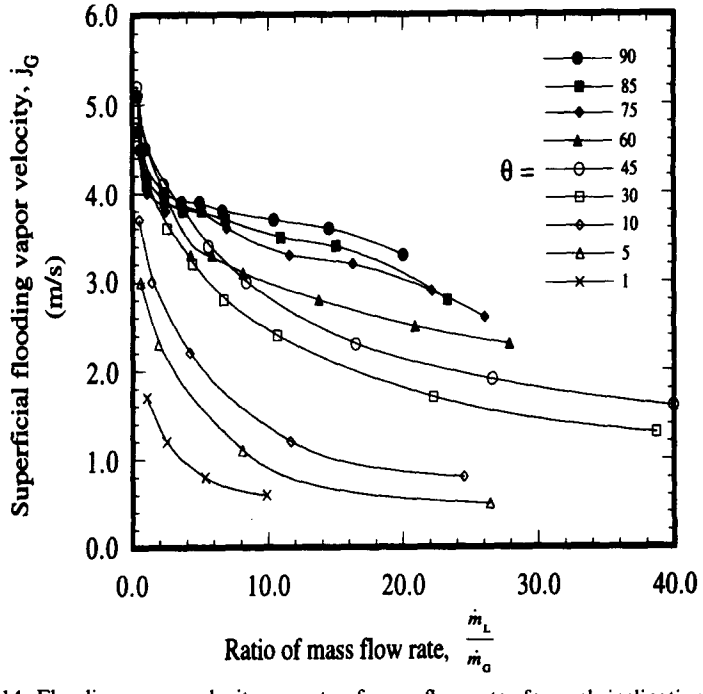

Figure 14. Flooding vapor velocity vs. rate of mass flow rates for each inclination angle.

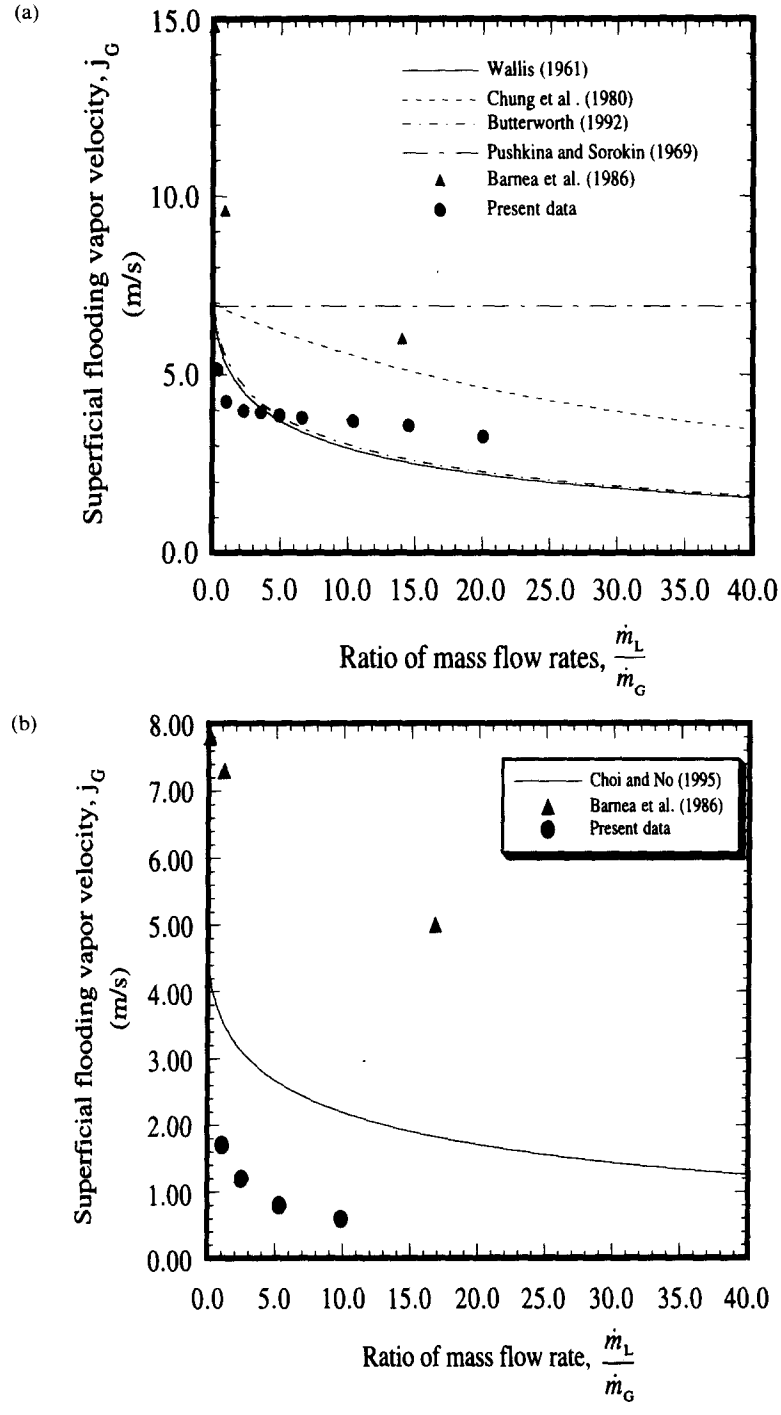

Figure 15. (a) Superficial flooding vapor velocity vs ratio of mass flow rates for the vertical position. (b) Superficial flooding vapor velocity vs ratio of mass flow rates for the nearly horizontal position.

Figure 15(a) and (b) show comparisons of the superficial flooding vapor velocity for the smooth tube from the literature and the fluted tube with an insert for vertical and nearly horizontal positions, respectively. Equation [18] was used in plotting the correlations of Wallis (1961), Butterworth (1992) and Choi and No (1995) while [19] was in Chung *et al.* (1980) and Pushkina and Sorokin (1969). Figure 15(a) shows that the superficial flooding vapor velocity decreases with an increase in the ratio of the mass flow rates. For the cases of smooth tubes, the flooding vapor velocity decreases continuously with the ratio of mass flow rate. However, the flooding vapor

velocity decreases very slowly beyond the ratio of 5.0. It should be noted that when the ratio is less than 5.0, the superficial vapor velocity for the fluted tube with a twisted insert is lower than that from Wallis (1961) for the smooth tube for a given ratio of the mass flow rates while it was always higher than that from Wallis (1961) for a given liquid flow rate. Data from Barnea *et al.* (1986) gives the most sensitive effect of the ratio of the mass flow rates on the flooding vapor velocity. Figure 15(b) also shows that the superficial flooding vapor velocity decreases with an increase of the ratio of the mass flow rates. For the nearly horizontal position, the superficial flooding vapor velocity for the fluted tube with an insert is always lower than that for the smooth tubes from Choi and No (1995) and Barnea *et al.* (1986) for both a given liquid mass flow rate and the ratio of the mass flow rates. Figure 15(a) and (b) can be used directly to determine the tube size to avoid the flooding phenomenon for a given ratio of the liquid mass flow rate to the vapor mass flow rate.

4. CONCLUSIONS

This paper analyzed the flooding mechanism in a fluted tube with a twisted insert for each inclination angle, and developed experimental correlations for the flooding data as a function of the inclination angle. The experimental data from this paper were compared with those for smooth tubes from the literature. The following are drawn as conclusions:

(1) Flooding initiated from the top for the inclination angles less than 60° while it started from the bottom of the tube for the angles larger than 60°.

(2) The fluctuation of the pressure drop was very strong when flooding started from the bottom while it was not as strong as that when it started from the top. This was because the fluctuation was caused by only the liquid carryover and flooding did not propagate to the bottom but remained near the top of the tube when it started from the top, while it was caused by both the liquid carryover and the flow fluctuation itself from the bottom when it started from the bottom.

(3) The effect of the position of the insert was not significant for the nearly horizontal tube while it was somewhat significant for the vertical tube.

(4) The superficial flooding vapor velocity for the nearly horizontal position is lower than that for the vertical position for a given mass flow rate of the liquid flow.

(5) For the fluted tube with an insert, the flooding vapor velocity is the highest between the inclination angle of 40° and 60° for the superficial liquid velocities less than or equal to 1.178×10^{-2} m/s. When the superficial velocity of liquid flow is higher than 1.178×10^{-2} m/s, the superficial flooding vapor velocity increases with an increase in the inclination angle.

(6) When the ratio of liquid mass flow rate to the vapor mass flow rate is less than 5.0 in vertical position, the superficial vapor velocity from the present data is lower than that from Wallis (1961) for a given ratio of the mass flow rates while it was always higher than that from Wallis (1961) for a given liquid flow rate. However, for the nearly horizontal position, the superficial flooding vapor velocity from the fluted tube with an insert is always lower than that for the smooth tubes from the literature for both a given liquid mass flow rate and the ratio of the mass flow rates.

(7) The following correlations were developed from the fluted tube with a twisted insert with an error band of ±10%

$$\sqrt{j_G^*} + m(\theta^*)\sqrt{j_L^*} = C\left(\frac{\sigma}{\sigma_w}\right)^n C_0(\theta^*) \quad \text{for 5–90° inclination angles}$$

$$\sqrt{j_G^*} + 2.944\sqrt{j_L^*} = 0.625 \quad \text{for nearly horizontal position (1° inclination angle),}$$

where m, C, n and C_0 are given in [7]–[9].

REFERENCES

Alekseev, V. P., Poberezkin, A. E. and Gerasimov, P. V. (1972) Determination of flooding rates in regular packings. *Heat Transfer Soviet Res.* **4**, 159–163.

Bankoff, S. G. and Lee, S. C. (1986) A critical review of the flooding literature. In *Multiphase*

Science and Technology, Vol. 2, ed. G. F. Hewitt, Delhaye and Zuber, Chapter 2, pp. 95–180, Hemisphere, New York.

Barnea, D., Yoseph, N. and Taitel, Y. (1986) Flooding in inclined pipes—effect of entrance section. *The Canadian Journal of Chemical Engineering* **64,** 177–184.

Boucher, D. F. and Alves, G. E. (1973) Fluid and particle mechanics. In *Chemical Engineers' Hand Book*, ed. R. H. Perry and C. H. Chilton, 5th Ed., Sec. 5. McGraw-Hill, New York.

Butterworth, D. (1992) Film condensation of pure vapor, Flooding phenomena. In *Hand Book of Heat Exchanger Design*, Chapter 2.6.2, ed. G. F. Hewitt. Begell House, New York.

Cetinbudaklar, A. G. and Jameson, G. J. (1969) The mechanism of flooding in vertical countercurrent two-phase flow. *Chemical Engineering Science* **24,** 1669–1680.

Choi, K. Y. and No, H. C. (1995) Experimental studies of flooding in nearly horizontal pipes. *International Journal of Multiphase Flow* **21,** 419–436.

Chung, K. S., Tien, C. L. and Liu, C. P. (1980) Flooding in two-phase counter-current flows, II. Experimental investigation. *Physicochem. Hydrodyn.* **1,** 209–220.

Clift, R., Pritchard, C. L. and Nedderman, R. N. (1966) The effects of viscosity on the flooding conditions in wetted wall columns. *Chemical Engineering Science* **21,** 87–95.

Dukler, A. E. and Smith, L. (1979) Two-phase interactions in countercurrent flow: Studies of the flooding mechanism. *NUREG*/CR-0617, Nuclear Regulatory Commission, Washington, D.C.

Garimella, S. and Christensen, R. N. (1995) Heat transfer and pressure drop characteristics of spirally fluted annuli: Part II—Heat transfer. *Journal of Heat Transfer* **117,** 61–68.

Govan, A. H., Hewitt, G. F., Richter, H. J. and Scott, A (1991) Flooding and churn flow in vertical pipes. *International Journal of Multiphase Flow* **17,** 27–44.

Herbine, G. S. and Perez-Blanco, H. (1995) Model of an ammonia-water bubble absorber. *ASHRAE Transaction* **101,** 1324–1332.

Hewitt, G. F. and Wallis, G. B. (1963) Flooding and associated phenomena in falling film flow in a vertical tube. AERE-R4022, UKAEA, Hartwell, U.K.

Imura, H., Kusuda, H. and Funatsu, S. (1977) Flooding velocity in a counter-current annular two-phase flow. *Chemical Engineering Science* **32,** 79–87.

Kang, Y. T. and Christensen (1994) Development of a counter-current model for a vertical fluted tube GAX absorber. *Proceedings of The International Absorption Heat Pump Conference*, ASME, AES-31, pp. 7–16.

Kang, Y. T., Chen, W. and Christensen, R. N. (1996) Development of design model for a rectifier in GAX absorption heat pump systems. *ASHRAE Transaction* **102,** 963–972.

Kawaji, M., Thompson, L. A. and Krisnan, V. S. (1991) Counter-current flooding in vertical-to-inclined pipes. *Exp. Heat Transfer* **4,** 95–110.

Lacy, C. E. and Dukler, A. E. (1994a) Flooding in vertical tubes—I: Experimental studies of the entry region. *International Journal of Multiphase Flow*. **20,** 219–233.

Lacy, C. E. and Dukler, A. E. (1994b) Flooding in vertical tubes—II: A film model for entry region flooding. *International Journal of Multiphase Flow* **20,** 235–247.

Lee, S. C. and Bankoff, S. G. (1983) Stability of steam–water counter-current flow in an inclined channel; flooding. *Journal of Heat Transfer* **105,** 713–718.

Maron, D. M. and Dukler, A. E. (1984) Flooding and upward film flow in vertical tubes—II: speculations on film flow mechanisms. *International Journal of Multiphase Flow* **10,** 599–621.

McQuillan, K. W. and Whalley, P. B. (1985) A comparison between flooding correlations and experimental flooding data for gas–liquid flow in vertical circular tubes. *Chemical Engineering Science* **40,** 1425–1440.

Moffat, R. J. (1988) Describing the uncertainties in experimental results. *Experimental Thermal and Fluid Science* **1,** 3–17.

O'Brien, S. A., Such, D. K. and Mills, A. F. (1986) The effect of liquid flow rate on flooding in vertical annular countercurrent two-phase flow. *International Journal of Multiphase Flow* **12,** 669–704.

Pushkina, O. L. and Sorokin, Y. L. (1969) Breakdown of liquid film motion in vertical tubes. *Heat Transfer Sov. Res.* **1,** 56–64.

Srinivasan, V. and Christensen, R. N. (1992) Experimental investigation of heat transfer and

pressure drop characteristics of flow through spirally fluted tubes. *Experimental Thermal and Fluid Science* **5,** 820–827.

Taitel, Y. and Barnea, D. (1982) A film model for the prediction of flooding and flow reversal for gas–liquid flow in vertical tubes. *International Journal of Multiphase Flow* **8,** 1–10.

Taitel, Y. and Dukler, A. E. (1976) A model for predicting flow regime transition in horizontal and near horizontal gas–liquid flow. *AIChE Journal* **22,** 47–55.

Tien, C. L., Chung, K. S. and Liu, C. P. (1980) Flooding in two-phase counter-current flows, I. Analytical modeling. *Physicochem. Hydrodyn.* **1,** 195–207.

Wallis, G. B. (1961) Flooding velocities for air and water in vertical tubes. UKAEA Report, AEEW-R123.

Wallis, G. B. (1969) *One-dimensional Two-phase Flow*, Chapter 11. McGraw-Hill, New York.